Journal of Building Engineering 88 (2024) 109186

Contents lists available at ScienceDirect

Journal of Building Engineering

journal homepage: www.elsevier.com/locate/jobe

Genetic programming to understand the influence of new sustainable powder materials in the fresh performance of cement pastes

Gemma Rojo-López, Belén González-Fonteboa *, Juan Luis Pérez-Ordóñez, Fernando Martínez-Abella

Universidade da Coruña (UDC), Civil Engineering School, Centro de Innovación Tecnolóxica en Edificación e Enxeñaría Civil (CITEEC), Campus Elviña S/n, La Coruña, 15071, Spain

ARTICLE INFO

Keywords:
Biomass ash
Granite powder
Metakaolin
Artificial intelligence
Parametric analysis

ABSTRACT

This study focused on pastes that incorporate metakaolin, biomass ash, and granite powder as supplementary cementitious materials to obtain specific expressions to predict rheological properties in pastes and to define the most appropriate dosage parameters using genetic programming. For this purpose, a dataset was developed following a central composite design, and some fresh properties were measured: Marsh cone and rheological properties, such as yield stress and plastic viscosity. The models generated by genetic programming presented robust statistical indices for the properties studied. The influence of supplementary cementitious materials on rheological properties was also analysed through a parametric analysis. After analysing the factors affecting paste rheology, it was concluded that the most important aspects affecting fresh behaviour were water demand and particle interaction, as well as the relation between both effects.

1. Introduction and objectives

Supplementary cementitious materials (SCMs) are a wide range of natural or, commonly, industrial by-products materials used to replace part of the clinker in the binder composition. In cement composition, clinker is responsible for most of its cost and carbon emissions, so reducing its content has the dual benefit of reducing both the cost of cement production and its environmental impact. In addition, the use of industrial by-products directly favours circular economy, thus giving new valuable uses to materials that otherwise would have to be processed and eliminated as waste [1]. In fact, the employment of supplementary cementitious materials to obtain quaternary binders reducing clinker content is an issue that is increasing attention in the research community [2–8]. The inclusion of novel raw materials will modify the performance of the concrete and mortars, which may provoke that traditional quality control methods are not suitable to fully characterize their behaviour. This is more likely when we deal with the fresh state. In this regard, rheology is known to be the most effective technique for characterizing the workability of cementitious composites.

Fonseca et al. [9] used rice husk ash, metakaolin, limestone filler and hydrated-lime type CH–I to produce ternary and quaternary binders. The findings demonstrated that, due to their higher specific surface areas, metakaolin and rice husk ash raise the viscosity of

* Corresponding author.
E-mail addresses: gemma.rojo@udc.es (G. Rojo-López), bfonteboa@udc.es (B. González-Fonteboa), juan.luis.perez@udc.es (J.L. Pérez-Ordóñez), fmartinez@udc.es (F. Martínez-Abella).

https://doi.org/10.1016/j.jobe.2024.109186
Received 11 December 2023; Received in revised form 26 February 2024; Accepted 28 March 2024
Available online 3 April 2024

self-compacting concrete. Moreover, the durability parameters were significantly improved with ternary and quaternary binders. Gesoğlu et al. [10] analysed the effect of using marble powder and limestone filler combined with fly ash in binary and ternary blended cements. They concluded that, when the substitution percentages are high, fresh properties (analysed using industrial tests) are negatively affected; however, the incorporation of fly ash might counteract this effect. Biricik et al. [11] assessed the rheological properties of binary binders containing recycled concrete powder, glass powder, marble powder, and limestone powder in two replacement ratios (25% and 35%). It was demonstrated that the use of these by-products might help in the design of mixtures that require a special fresh behaviour in terms of rheology or thixotropy.

All these works show that many new supplementary cementitious materials are being explored in the research community, however, the ones employed in the work, such as biomass ash from the forest industry or granite powder from the ornamental stone industry, have not been widely studied. In addition, it is also seen that the literature works that employ rheology as a tool to better understand and define the fresh behaviour of novel quaternary binders is scarce. The combination of novel SCM with the use of rheology to characterize the fresh behaviour is a novelty that may contribute to widespread the use of this new by-products.

This new opportunity to advance in the sustainability offered by by-products requires an effort prior to their widespread use in the construction industry. Extensive experimental campaigns must be performed to analyse the effects of by-products on the properties of cement-based mixtures in both the fresh and hardened states. Durability studies are also essential for the successful use of by-products. These extensive experimental campaigns consume much time and resources, so they should be optimally designed.

One suitable option is the analysis at paste level, which requires less material, permits the variation of many parameters, and avoids the effect of aggregates. The use of techniques as Design of Experiments (DOE) to optimize the experimental campaigns are also recommended. In addition, to develop the data treatment, the most interesting possibility relies on knowledge extraction techniques based on machine learning (ML) or artificial intelligence (AI). If these techniques are accurately used, useful and efficient models could be developed to predict fresh or hardened properties.

All this is especially recommended when studying fresh behaviour because, as it is well-known, concrete and mortar can be considered as suspensions where the solid phase is the aggregate, and the liquid phase is the cement paste. The concrete/mortar fresh behaviour at the level of cement paste can be therefore studied, as well as the influence of the aggregate incorporation can be then analysed. In all cases, the influence of all mix design parameters on cement paste behaviour should be known, and the relationship between paste properties and mortar/concrete behaviour should be assessed.

Some research works can be found in the literature that employ DOE in the mixture design when SCMs are used replacing clinker with the aim of producing more sustainable concretes [12–15]. Nunes et al. [13] investigate the viability of using recycled ground glass powder in percentages that range from 22% to 47%. The same authors revealed [12] that spent equilibrium catalyst, which is a waste generated by the oil refinery industry, can be used in a high percentage to obtain self-compacting mortars due to its high pozzolanic activity. Matos et al. [14] have selected a ternary blended cement of white Portland cement, limestone filler and metakaolin to produce a white self-compacting high performance concrete. Many of these works use central composite design (CCD) to study the hardened behaviour, while the analysis of the rheological performance is scare [16,17].

In the field of structural and material engineering, machine learning techniques to generate more accurate and reliable models have been effectively used. A machine learning technique based on artificial intelligence predicts outcomes by using a database. Examples of the employment of these techniques, focused on predicting the hardened concrete properties, are commonly found in the literature. [8, 18–24], and researchers have progressively introduced these statistical techniques to forecast the rheological properties of concrete [25–27].

Navarrete et al. [26] evaluated the static yield stress of cement pastes containing inert filler, class C and class F fly ash, rice husk ash, and metakaolin as SCMs through three machine learning methods: multilayer perceptron (MLP), random forest (RF), and support vector machine (SVM), although genetic programming is not used in the work. These three methods achieved good results in the training phase, but MLP showed the highest R^2 and the lowest root mean square error (RMSE) in the testing phase. ML was therefore a good option for modelling cementitious materials properties.

Al-Martini and Nehdi [28] used genetic algorithms to adjust shear stress versus shear rate for cement pastes by incorporating various superplasticisers at different temperatures and mixing times. The rheological parameters of the Bingham model were obtained from these curves, and the values of yield stress and plastic viscosity calculated by the algorithms fit accurately the experimental data. This work deals specially with the effect of superplasticisers and the cement employed is a clinker Portland cement.

Figueiras et al. [29] stated that the prediction of concrete or mortar behaviour based on paste characteristics allows self-compacting concrete mix design to be simplified. Two statistical experimental designs were developed: one at paste level, and the other at mortar level. Afterwards, numerical models were adjusted by using multivariable regression to analyse the influence of various mixing parameters on fresh and hardened properties. Finally, an area was defined at paste level to design self-compacting mortar saving time, materials, and effort. This work employs ternary binders with limestone filler and metakaolin.

Various smart techniques can be used to know the behaviour of cement-based material. Taking into account the characteristics of the ML techniques [19,30,31], genetic programming was chosen as the most suitable technique as it allows an explicit mathematical equation to be adjusted to also adjust the design variables of new mixtures based on these prediction models [21], as well as complex properties considering many variables to be modelled [23].

As was seen, the combination of DOE and genetic programming to study the rheological behaviour of cement-based materials with quaternary that incorporate novel SCM binders (biomass ash, metakaolin and granite powder) is a novelty that must be explored. Considering the research potential at paste and mortar level, this work proposes a wide experimental campaign that designs pastes and mortars using the same raw materials and incorporates various by-products as supplementary cementitious materials. The fresh behaviour of mortars mixes has been previously analysed [32,33], so this study aimed to state that genetic programming could be used

to predict the fresh behaviour of cement-based pastes. It also aimed to show that the influence of quaternary binders incorporating various sustainable by-products in the fresh behaviour of the paste can be assessed by using genetic programming and throughout a parametric analysis. The influence of both the main mixing parameter and the new by-products could be understood by using mathematical models obtained by genetic programming.

The final objective is to confirm that the mathematical models adjusted to predict the fresh behaviour of the paste and those fitted to predict the behaviour of the mortar [33] can be used to establish suitable relationships between some of the most important fresh state parameters: the Marsh cone time of the paste vs the Tfunnel of the mortar, and the yield stress of the paste vs the yield stress of the mortar. These relationships are used to understand the influence of paste composition (especially the volume and the type of the by-products used to design the quaternary binder) on fresh mortar properties.

2. Experimental programme

2.1. Materials and mixes

Portland cement labelled as CEM I 52.5 N-SR5 (CEM), metakaolin (MK), granite powder (GP) and biomass ash (BA) were used. Table 1 presents the chemical properties of the powder materials.

Figs. 1 and 2 show the gradation of the powder materials measured by laser diffraction and SEM images. While biomass ash and granite powder were coarser and finer than cement, respectively, cement and metakaolin exhibited a similar degree of fineness.

Granite powder was a by-product of the extraction and manufacture of granite rocks, while the biomass ash used in this work was a by-product of the wood sector [33]. Moreover, metakaolin was used as a pozzolanic material (Table 2 includes its physical properties). Likewise, tap water and a polycarboxylate-based superplasticizer were used in the mix design.

Twenty-five paste mixes were designed using the blended cements. The paste mix design was based on the central composite design (CCD) plan used in a previous study to analyse self-compacting mortar workability [33]. The same independent variables, showed in Table 3, were used. Additionally, a set weight ratio between metakaolin and cement (mk/c = 0.20) was established. These variables, together with the packing density, were used to develop the genetic programming training. The mix composition of the pastes obtained with the CCD plan is included in Table 4.

2.2. Testing protocols

Paste mixes were prepared in 1.7 l batches and were mixed in a mixer according to EN 196–1 [36]. The batching protocol is displayed in Fig. 3.

Powder materials were mixed with 80% of mixing water at a slow, continuous speed (140 ± 5 rpm) for 1 min. The rotation was then stopped to remove the material stuck to the container walls and restarted for 1 min. Afterwards, the superplasticizer and the remaining water were incorporated. The paste was mixed for two additional minutes, then resting for 2 min. Finally, the paste was mixed for an additional period of 2 min at a high speed (285 ± 10 rpm).

One empirical and two rheological tests were carried out to characterize the fresh state of the pastes. The empirical test was the Marsh cone, i.e., a workability test applied to cement paste [37] and developed according to the standard [38] to obtain the time in seconds needed for an amount of paste to flow through the cone. In parallel, the rheological characterisation was carried out with the Viskomat NT, which is a rotational rheometer with a window vane (Fig. 4) and whose geometry is adapted to the maximum particle size of solid materials.

The stress growth test (SGT) and the flow curve test (FCT) [39] were used. Table 5 defines the main testing parameters.

The yield stress (Pa) and the plastic viscosity (Pa s) of the pastes were measured with these two testing protocols. Both parameters were measured for 30 min after water-cement contact. Viskomat NT measured parameters in relative units, and the conversion to absolute parameters was obtained by applying the integration approach of the Couette inverse problem of Herschel-Bulkley fluid [21]. The plastic viscosity value was obtained in absolute units from the FCT by applying the Herschel-Bulkley model, thus obtaining the value for a speed of 100 rpm. Likewise, the yield stress value was obtained from the SGT using the torque value when it was stabilised during the test. The yield stress was obtained as an average value of 5 s (Fig. 5).

3. Genetic programming

The genetic programming technique was used to analyse the rheological behaviour results obtained by the experimental programme. This technique is included in an AI sub-branch called evolutionary computing, which is based on search techniques inspired by the evolution of species. According to Darwin's theory of evolution, the better adapted individual is more likely to perpetuate itself (the principle of natural selection of species) [40]. The problem to be solved represents the environment, and the set of solutions represents the different individuals that adapt to the environment. Solutions (individuals) are represented by a tree structure with two

Table 1
Chemical composition of the powder materials (% by weight).

	SiO_2	Al_2O_3	Fe_2O_3	CaO	K_2O	Na_2O	MgO	SO_3	LOI
CEM	18.9	6.3	2.7	59.9	1.9		1.6	3.5	4.3
BA	40.0	16.6	5.5	10.2	6.9	1.6	2.8	2.4	2.7
GP	70.4	15.2	2.0	1.0	5.5	3.7	0.35		1.0
MK	58.0	36.8	1.2	0.075	2.1		0.18	0.058	0.7

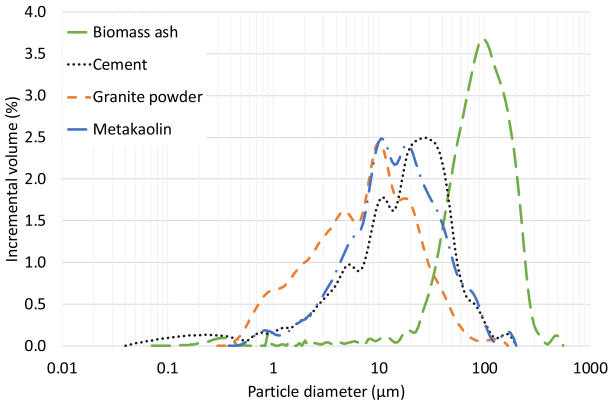

Fig. 1. Grading curves of the powder materials.

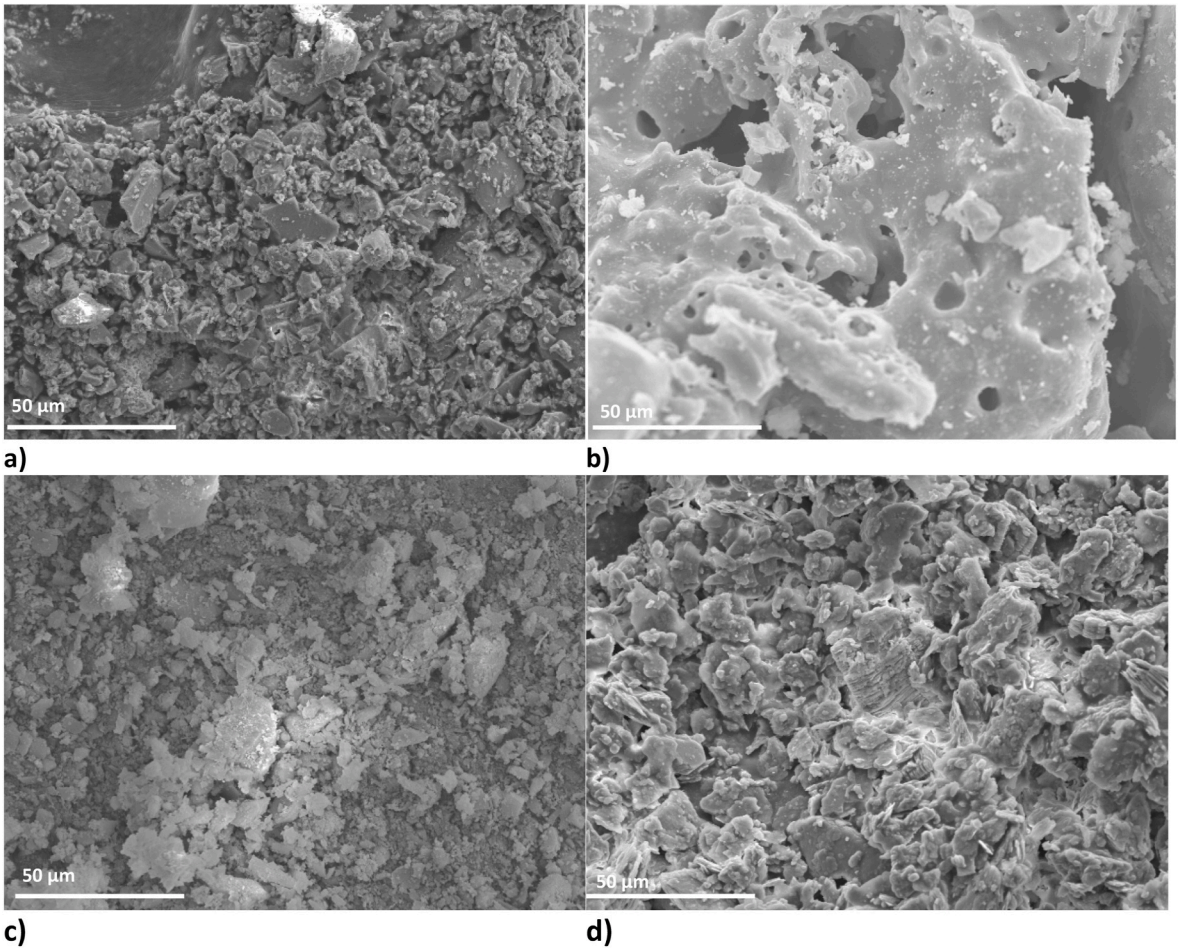

Fig. 2. SEM images: a) CEM. b) BA. c) GP. d) MK.

types of nodes: 1) non-terminal nodes (functions) where the operators of the algorithm are stored (e.g., addition, multiplication, and so on), and 2) terminal nodes or tree leaves, where the constant values and the previously defined variables are located [41].

PG operates as follows: a set of solutions (population) is randomly generated, and its adaptation to the environment (fitness function) is evaluated. In the next iteration, new individuals are created from the individuals of the previous iteration by using selection, mutation, and crossover algorithms. The set of individuals generated in each iteration is called generation.

Table 2
Physical properties.

	CEM	BA	GP	MK
Specific density (g/cm^3)	3.04	2.68	2.77	2.55
Particle density - N_{PSD} [27]	23	19	40	1
Packing [34]	0.48	0.45	0.39	0.30
Pozzolanic activity (mg of $Ca(OH)_2$) [35]		258	48	946

Table 3
Range of the independent variables used in the mortar and paste mix design.

Independent variables	Range
V_w/V_p	0.75–0.95
w/c	0.4–0.6
Sp/p	0.015–0.017
ash/c	0.1–0.2

Where.
V_W/V_P: water to powder volume ratio w/c: water to cement weight ratio.
Sp/p: superplasticizer to powder weight ratio ash/c: biomass ash to cement weight ratio.

Table 4
Paste mixes (kg/m^3).

	Paste mixes					
Ref	CEM	MK	BA	GP	Sp	Water
Ci (i = 1–6)	1556.14	311.23	233.42	535.86	42.19	744.45
F1	1672.55	334.51	209.07	500.01	42.10	719.09
F2	1782.91	356.58	222.86	224.78	40.10	770.35
F3	1368.49	273.70	171.06	882.27	41.78	719.37
F4	1458.79	291.76	182.35	632.26	39.76	770.65
F5	1672.14	334.43	209.02	499.89	44.81	716.75
F6	1782.49	356.50	222.81	224.73	42.68	768.11
F7	1368.15	273.63	171.02	882.05	44.47	717.05
F8	1458.45	291.69	182.31	632.11	42.32	768.42
F9	1672.56	334.51	292.70	413.77	42.06	719.13
F10	1782.92	356.58	312.01	132.85	40.06	770.39
F11	1368.50	273.70	239.49	811.70	41.75	719.40
F12	1458.80	291.76	255.29	557.03	39.72	770.68
F13	1672.14	334.43	292.63	413.66	44.76	716.79
F14	1782.50	356.50	311.94	132.82	42.63	768.15
F15	1368.16	273.63	239.43	811.50	44.43	717.08
F16	1458.46	291.69	255.23	556.90	42.28	768.46
CC1	1451.23	290.25	217.68	814.57	44.38	690.25
CC2	1650.32	330.06	247.55	285.64	40.22	793.11
CC3	1945.10	389.02	291.76	36.84	42.60	744.08
CC4	1296.82	259.36	194.52	868.56	41.91	744.69
CC5	1556.51	311.30	233.48	535.99	39.56	746.73
CC6	1555.76	311.15	233.36	535.73	44.81	742.17
CC7	1556.13	311.23	155.61	616.10	42.23	744.41
CC8	1556.14	311.23	311.23	455.62	42.15	744.48

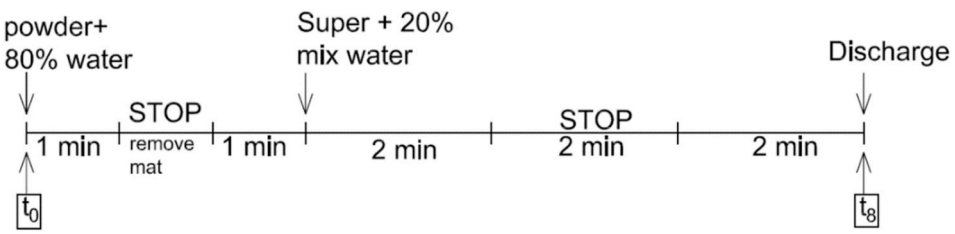

Fig. 3. Paste mixing procedure.

Fig. 4. Paste rheometer and window vane.

Table 5
Rheological testing parameters in SGT and FCT.

	Speed (rpm)	Breakdown time (s)	Steps
SGT	6	–	–
FCT	140	20	7

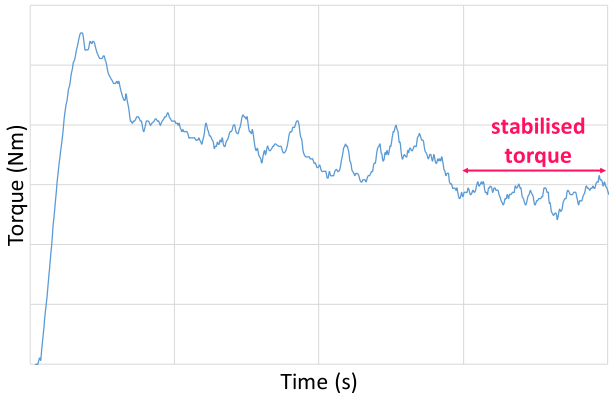

Fig. 5. Time vs Torque SGT test.

The process ends when a termination criterion is reached: 1) when the required fit is obtained, or 2) when the maximum set number of generations is reached. More information on this technique can be found in Pérez et al. [20].

3.1. Genetic programming settings

After performing the initial tests, the following default parameters were set: Population 1000 individuals, 80% crossover rate, 20% mutation probability, and 90% Non-terminal selection rate. The algorithms used were as follows: "tournament" for selection, "intermediate" for crossover creation, and "subtree" for mutation. Likewise, an elitist approach was used: if no individual with the best fit was obtained, the best individual from the previous generation would be retained. The parsimony factor was set to 0.001, and the maximum tree size was limited to 9 nodes deep to obtain easy expressions. The initial tree size and the maximum position for mutation were set at 6 nodes.

The addition, subtraction and product operators were chosen as non-terminal nodes. Likewise, the design variables included in Table 3 (Vw/Vp, w/c, Sp/P, and ash/c) and integer numbers were set for terminal nodes. Free programming was first used to obtain the equation that predicted the values of the properties. After analysing the results, two good equations were found for Mash cone time (MC) and yield stress (YS), unlike for plastic viscosity (PV), so an equation structure was used as a guide as follows:

$$PV_{PG} = \frac{Branch_0}{Branch_1} \bullet \left(\frac{V_W}{V_P}\right)^{Branch_2} \quad \text{Eq. 1}$$

The following constrains were set for each branch.

- Branch$_0$: it could contain any input variable and the addition, subtraction, and product operators (non-terminal nodes).
- Branch$_1$: it could contain any input variable, avoiding V_W/V_P, as well as the addition, subtraction, and product operators.
- Branch$_2$: it was a constant greater than 2.

The performance of the final models was checked by measuring four statistical indicators: 1) the mean square error (MSE), 2) the mean error (MAE), 3) the square of the Pearson product-moment correlation coefficient (R2), and 4) the coefficient of variation (COV) [20].

3.2. Paste datasets

The paste dataset was the result of the experimental campaign. Data (Table 6) were divided into two sets: 27 paste mixes were used for training, and the remaining 3 for testing. Given the intrinsic error associated to the test, Ci mixes with identical input variables gave different output outcomes.

4. Adjusted equations

The free genetic programming was applied to the results obtained by the Marsh cone test, thus obtaining Eq. (2):

$$MC_{PG} = \left(7 \cdot \frac{w}{c} + 8\right) \cdot \left(8 \cdot \frac{w}{c} + 6\right) + \frac{4}{5 \cdot \left(\frac{Vw}{Vp} - \frac{10}{13}\right)} - 11 \cdot \frac{\frac{Vw}{Vp} - \frac{11}{13}}{\frac{Sp}{P}} \quad \text{Eq. 2}$$

The variables involved in the equation were three of the five input variables, thus indicating that the influence of both ash/c and the dry packing fraction (variables not considered in the equation) was slight. Both V_w/V_p and w/c were the most present variables, as in the prediction of the Tfunnel of the mortar [32].

Likewise, plastic viscosity (PV) and yield stress (YS) were obtained from the rheological tests. The equations adjusted to predict these two parameters using genetic programming are Eq. (3) by guided genetic programming, and Eq. (4) by free genetic programming, respectively.

Table 6
Paste dataset.

	Code	Marsh cone time (s)	Plastic Viscosity (Pa s)	Yield Stress (Pa)
Training	C1	125.0	5.50	2.81
	C2	125.5	4.83	2.69
	C3	128.5	7.04	2.99
	C4	129.0	5.92	3.05
	C5	119.5	5.52	3.19
	F1	180.5	11.15	4.25
	F2	80.5	2.71	2.01
	F3	177.0	9.54	4.56
	F4	94.5	3.67	2.02
	F5	160.0	12.14	4.41
	F6	74.5	2.45	1.81
	F7	192.0	8.46	4.44
	F8	89.0	3.48	1.79
	F9	174.5	8.10	4.51
	F10	71.5	2.12	1.86
	F12	89.0	3.11	1.93
	F13	158.0	7.50	4.19
	F14	69.0	2.11	1.77
	F15	172.0	9.66	4.43
	F16	115.0	3.89	2.36
	CC2	48.5	1.32	1.11
	CC4	132.5	7.07	2.86
	CC5	117.0	5.38	2.95
	CC6	117.5	5.48	2.69
	CC7	127.5	6.71	2.79
	CC8	99.5	3.36	2.10
Test	C6	129.0	5.91	3.09
	F11	171.5	8.70	5.16
	CC3	97.5	3.93	2.87

$$PV_{PG} = \frac{\text{Branch}_0}{\text{Branch}_1} \cdot \left(\frac{Vw}{Vp}\right)^2$$

Where:

$$\text{Branch}_0 = \left(1 - \frac{Vw}{Vp}\right) \cdot \left(\left(1 - \frac{Vw}{Vp}\right) \cdot (54 - Packing) \cdot \left(10 \cdot \frac{ash}{c} + 6\right) + 336 \cdot \left(1 - 2 \cdot \frac{w}{c}\right) \cdot \left(-2 \cdot \frac{Sp}{p} - 9 \cdot \frac{ash}{c} + 1\right) - 3\right) \quad \text{Eq. 3}$$

$$\text{Branch}_1 = \frac{ash}{c} \cdot \left(-12 \cdot \frac{ash}{c} + 24 \cdot \frac{w}{c} - 3\right)$$

$$YS_{PG} = -125 \cdot \frac{Sp}{p} + \left(\frac{Sp}{p} + \left(\frac{7}{2} - 4 \cdot \frac{Vw}{Vp}\right) \cdot \left(9 \cdot Packing - 4 \cdot \frac{Vw}{Vp}\right)\right) \cdot \left(-558 \cdot Packing - 18 \cdot \frac{w}{c} + 262\right) + 4 \quad \text{Eq. 4}$$

Both equations were structured as a sum of variables operators with linear and quadratic interactions of the independent variables. All the independent variables were used to predict plastic viscosity. To predict the yield stress, however, the biomass ash to cement ratio was discharged, and it was not used in the equation. Again, as expectable, V_w/V_p was the most used variable to predict PV and YS.

Fig. 6, Fig. 7, and Fig. 8 show the correlation between the values experimentally measured and the values obtained by applying the adjusted equations. According to the statistical indicators (Table 7), all the equations were suitable to predict the parameters accurately as V_{exp}/V_{pred} were always close to 1, ECM values were low, and R^2 was high.

5. Parametric analysis

The equations adjusted using genetic programming can be used to study the influence of the independent variables on the fresh state properties of the paste by developing a parametric analysis. To do that, the equations were parametrised as a function of $(V_{CEM} + V_{MK})/V_P$, V_{GP}/V_P, V_{BA}/V_P so that it was possible to analyse the influence of each powder material on the paste properties separately.

The effect of the active powder volume ($V_{CEM} + V_{MK}$) on the studied properties was analysed by maintaining the V_{BA}/V_{GP} constant equal to 1 in Figs. 9 and 10.

Active powder volume is an important parameter that highly controls water demand and consequently influences mixture rheology. In Fig. 9, when water volume was low ($V_W/V_P = 0.78$), the effect of increasing the active powder volume reduced Marsh cone time by 7.3%. When the amount of water was high (a V_W/V_P ratio of 0.94), reductions increased, reaching 29.4%. In any case, when the active powder volume was increased, Marsh cone time was reduced.

However, the effect of active powders on the yield stress was different (Fig. 10). The yield stress slightly increased by increasing active powders (4.3% when V_W/V_P was low, and only 1.3% when V_W/V_P was high). This parameter was more affected by water demand than Marsh cone time, which explains the yield stress increase when $V_{CEM} + V_{MK}/V_P$ rose.

The interaction among particles is an important issue influencing fresh paste behaviour. The reductions in water demand, which greatly depend on the quantity of active powders, and the interaction among particles with bad geometries (in terms of shape and texture) had opposite effects. Yield stress was more influenced by the former, while Marsh cone time was influenced by the latter.

In this work, when the active powder volume decreased (i.e., the volume of materials with bad geometries, such as biomass ash and granite powder, increased), the time in the Marsh cone test increased. Less active powder volume meant a reduction in water demand, but the effect of the particle interaction on Marsh cone time was predominant. In other words, the volume of biomass ash and granite powder negatively affected Marsh cone results. This was also detected in the parametric analysis of the Tfunnel measured in the mortar mixes [33].

On the other hand, when the volume of biomass ash and granite powder increased (i.e., less active powder volume), the value of yield stress decreased. Hence, this parameter was more influenced by the effect of water demand than Marsh cone time.

The influence of the volume of biomass ash and granite powder is shown in Figs. 11 and 12 where $(V_{CEM} + V_{MK})/V_{GP}$ was kept fixed

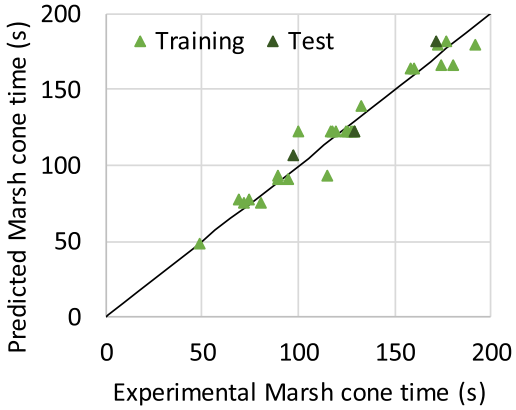

Fig. 6. Experimental vs predicted Marsh cone time (MC).

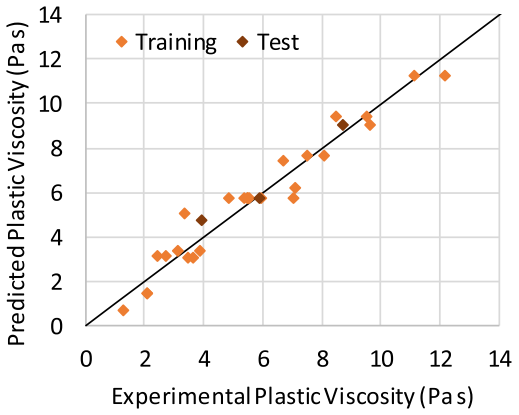

Fig. 7. Experimental vs predicted values (PV).

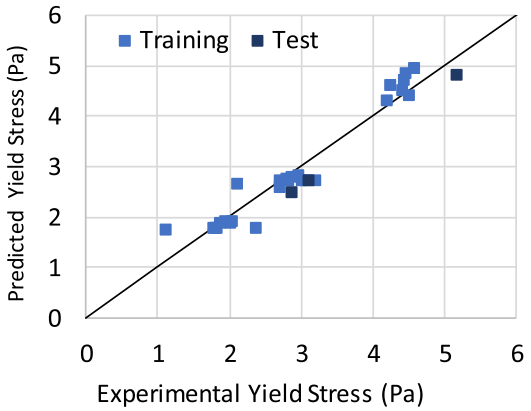

Fig. 8. Experimental vs predicted values (YS).

Table 7
Statistical indices.

	PV	YS	MC
COV	21.99	11.82	7.45
V_{exp}/V_{pred}	1.04	1.02	1.00
Max (exp/pred)	1.85	1.31	1.23
Min (exp/pred)	0.67	0.63	0.81
R^2	0.94	0.96	0.95
ECM	0.44	0.10	73.00
EM	0.56	0.24	6.77

at 3 (the effect of biomass ash varying active powder and granite powder), as well as in Figs. 13 and 14 where $(V_{CEM} + V_{MK})/V_{BA}$ was kept fixed at 7 (the effect of granite powder varying active powder and biomass ash).

In Fig. 11, Marsh cone time increased by increasing biomass ash (V_{BA}/V_P) from 0.07 to 0.13 (thus reducing active powder and granite powder). In Fig. 13, the same property is increased by increasing granite powder (V_{GP}/V_P) from 0.11 to 0.36 (thus reducing active powder and biomass ash). Increases were always greater with the increase in granite powder than in biomass ash. When the amount of water was low ($V_W/V_P = 0.78$), the increase was 2.1% (effect of biomass ash) or 11.0% (effect of granite powder). When water content was high ($V_W/V_P = 0.94$), these percentages were 8.8% and 38.9%, respectively. As discussed previously, the reduction of active powders reduced mixture water demand. However, as this reduction increased biomass ash or granite powder, Marsh cone time increased. This indicates that the effect of particle interaction, given the bad geometrical characteristics of the particles of the inert powders, dominated Marsh cone time behaviour even when the amount of water was high. The reduction in water demand associated with lower volume of active powders was counteracted by the interaction among particles with bad geometrical properties of biomass ash and granite powder.

This trend was different when the yield stress was analysed (Figs. 12 and 14). Yield stress was controlled by water demand. Therefore, the yield stress slightly decreased when biomass ash increased (1.8% when V_W/V_P was low, and 3.9% when V_W/V_P was

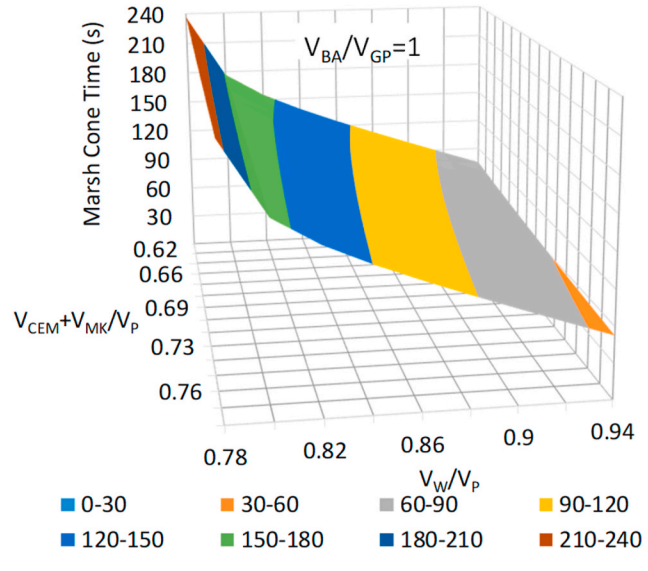

Fig. 9. $(V_{CEM} + V_{MK})/V_P$ influence on Marsh cone.

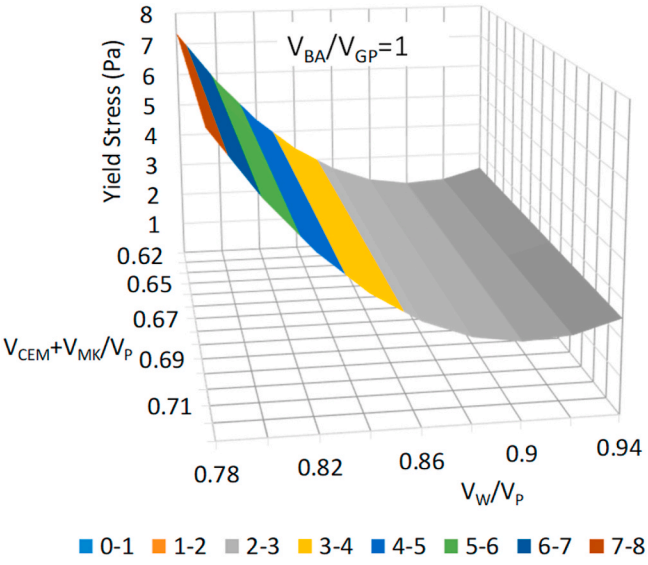

Fig. 10. $(V_{CEM} + V_{MK})/V_P$ influence on yield stress.

high). Increasing granite powder also decreased the yield stress slightly (3.9%) when water content was low, but when water content was high, as water demand was not a problem, the negative effect of the bad particles introduced by granite powder was so important that the yield stress increased (19.9%). In other words, the negative effect of including granite powder with irregular particle shapes and higher fineness than cement and metakaolin dominated behaviour.

Finally, Figs. 15 and 16 were developed to examine the impact of GP better when compared to the impact of biomass ash on both Marsh cone time and the yield stress. The active powder volume ($V_{CEM} + V_{MK}/V_P$) was maintained fixed at 0.74, and the inactive powder volume was also kept constant ($V_{BA} + V_{GP}/V_P = 0.244$). Nevertheless, the V_{BA}/V_{GP} relationship varied between 0.2 and 2.3.

Fig. 15 shows that increasing water volume reduced Marsh cone time to 74% regardless of the amounts of inactive powders.

Fig. 16 shows that the yield stress was positively affected by increasing the biomass ash volume (which meant that granite powder content dropped). Increasing biomass ash reduced the variable to 5.3% (when water volume was low), and to 18.1% when water volume was high. The negative effect of the particle shape of granite powder (finer than the other powders and with very bad geometrical properties) was higher when water content was low.

To sum up, Marsh cone time was more affected by the bad geometrical properties of the powder particles than by water demand, so it increased when the granite powder or biomass ash volume increased. On the contrary, the yield stress was more affected by water

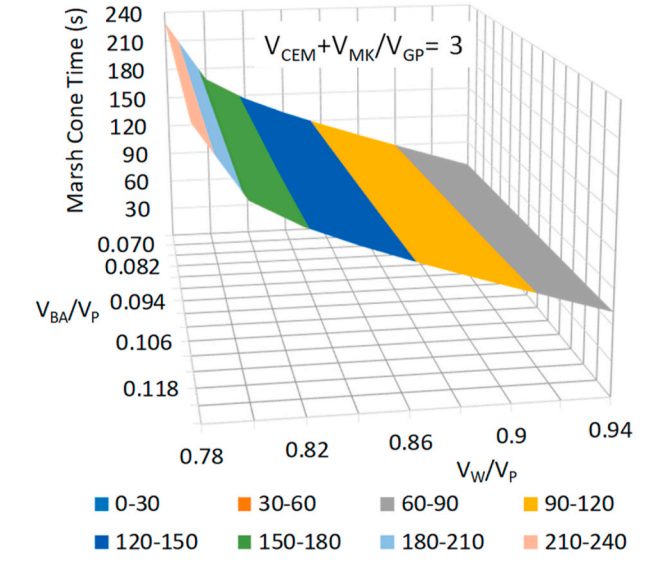

Fig. 11. V_{BA}/V_P influence on Marsh cone.

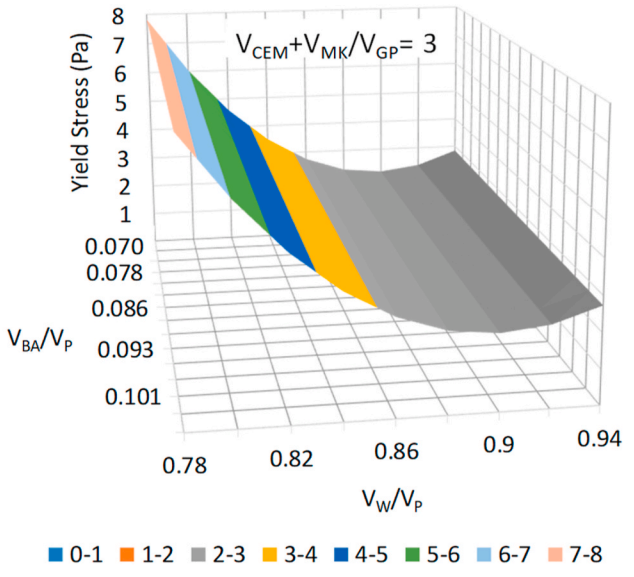

Fig. 12. V_{BA}/V_P influence on yield stress.

demand, so it increased when the ratio V_{CEM} + V_{MK}/V_P increased. Granite powder, with particles with worse geometrical properties than biomass ash, affected the fresh properties of the paste more negatively than biomass ash.

The influence of V_{CEM} + V_{MK}/V_P on the viscosity values was analysed (Fig. 17): when water volume was high (V_W/V_P is 0.94) by increasing active powder volume, the viscosity value was reduced by 72.6%. In this case, as water demand was not a problem, increasing active powders (thus reducing the ones with particles with bad geometrical properties, i.e., BA and GP) reduced viscosity. However, when water volume was low (V_W/V_P is 0.78), the increase of active powders led the viscosity to 13 Pa s (which meant an increase of about 41.0%).

In Fig. 18, the changes in the viscosity when biomass ash was modified (changing active powder and granite powder volume) were analysed. According to the previous result, when water volume was high, increasing biomass ash increased the viscosity. This is because the effect of water demand was removed and the effect of the particle shape is the one that dominated the behaviour. When water volume was low, when biomass ash was increased (that meant a reduction in active powder and granite powder), plastic viscosity values were reduced by 59.8% because water demand was also being reduced.

Fig. 19 shows the effect of granite powder on the viscosity. In this case, viscosity always rose when granite powder content

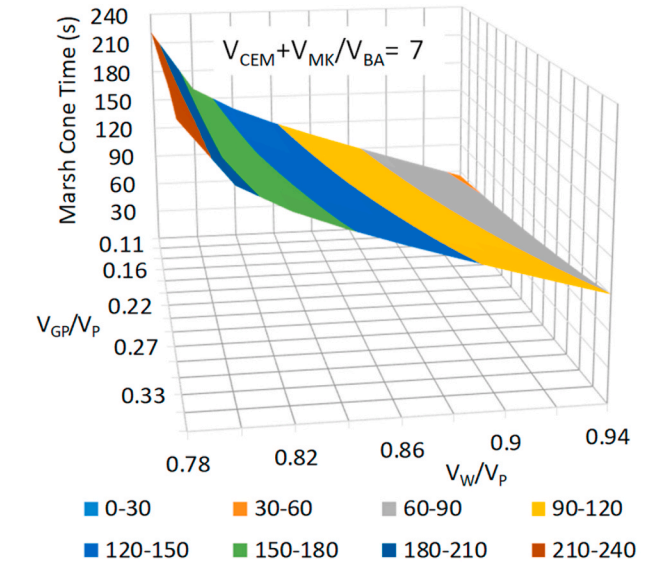

Fig. 13. V_{GP}/V_P influence on Marsh cone.

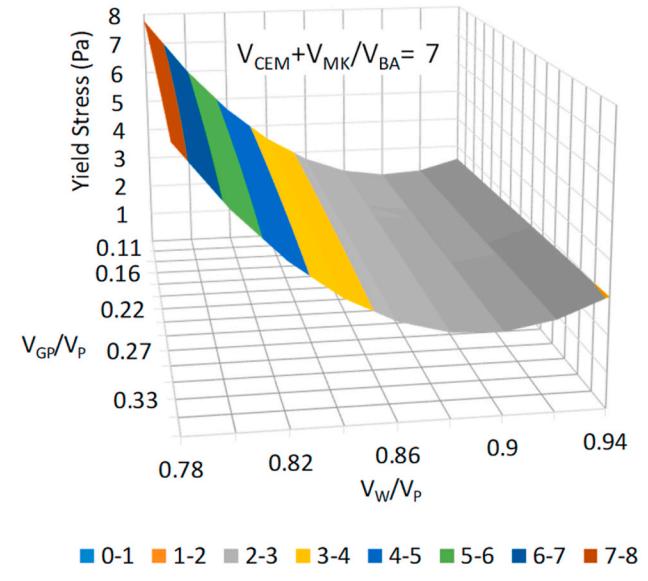

Fig. 14. V_{GP}/V_P influence on yield stress.

increased. When water content was high, increases were around 55.3%, as well as 0.6% when water content was low.

Fig. 20 was developed to better examine the impact of GP on plastic viscosity when compared to the impact of biomass ash. The active powder volume ($V_{CEM} + V_{MK}/V_P$) was fixed at 0.74, and the inactive powder volume was also constant ($V_{BA} + V_{GP}/V_P = 0.244$). Nevertheless, the V_{BA}/V_{GP} relationship varied between 0.2 and 2.3.

The plastic viscosity was positively affected by the increase in biomass ash (which meant that granite powder content dropped). Increasing biomass ash when water volume was low significantly reduced the variable from 32 to 4 Pa s (86.1%). When water content was high, the plastic viscosity was reduced by 2.8%.

Finally, all figures show that, regardless of the composition of the binder, when water volume was modified, all fresh parameters changed sharply, thus indicating that this is the most important parameter affecting fresh behaviour.

Table 8 summarises how the water volume and the variation in the volume of the powder materials used as by-products in the binder composition affect properties. Slight variations are shown by a single arrow, and great variations are shown by a larger arrow. Moreover, the percentage of variation is indicated.

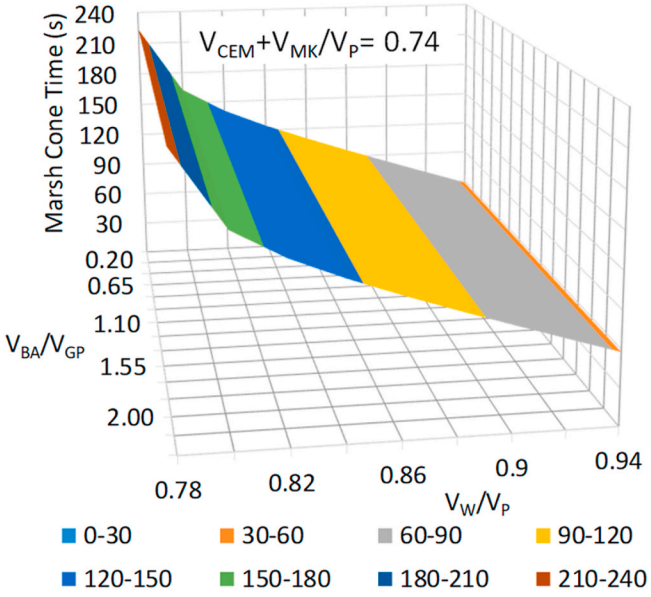

Fig. 15. V_{BA}/V_{GP} influence on Marsh cone.

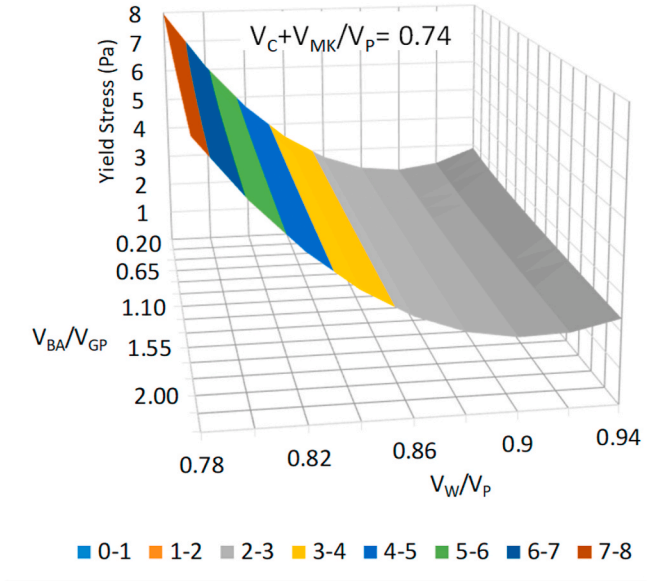

Fig. 16. V_{BA}/V_{GP} influence on yield stress.

Marsh cone time was highly affected by the particle interaction, so it should be reduced by reducing powder materials with particles with bad geometrical properties, angular shape, or rough texture, even if active powder materials increase (in water demand).

The yield stress was more affected by water demand, so it generally decreased when active powers dropped (inert powders growth). However, when water content is low, the yield stress is reduced regardless of whether biomass ash of granite powder are replacing active powders. On the contrary, when water content was high, and water demand is not a problem, using biomass ash to replace active powder reduced the yield stress, while using granite powder increased the yield stress.

By analysing viscosity, it is seen that, when water content was low, the effect of water demand was dominating, so decreasing active powders generally decreased viscosity. This occurred when active powders were replaced by biomass ash; however, when granite powder was used as a substitute, the viscosity slightly increased. If water volume was high, decreasing the active powder volume (increasing particles with bad geometrical properties, either BA or GP) increased the viscosity value, which meant that this parameter was more affected by the particle interaction than yield stress.

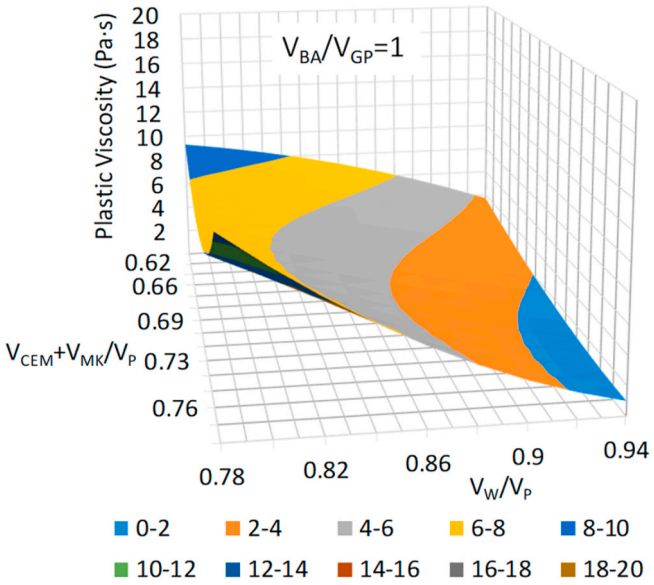

Fig. 17. $(V_C + V_{MK})/V_P$ influence on plastic viscosity.

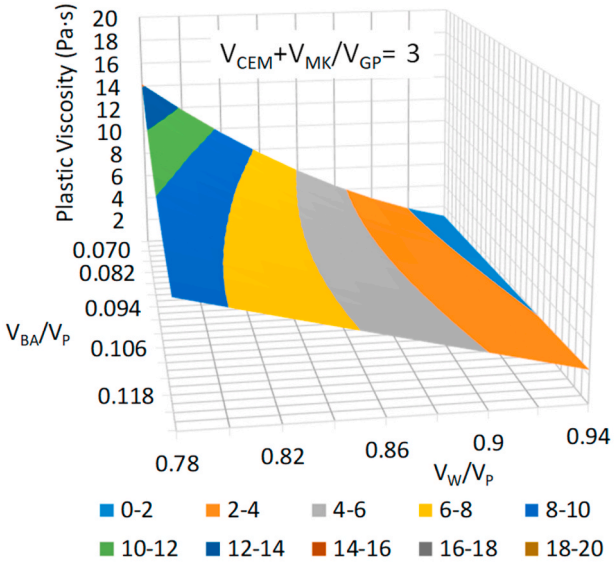

Fig. 18. V_{BA}/V_P influence on plastic viscosity.

6. Paste – mortar relationship

The relationship between paste and mortar rheological parameters was analysed by using the equations adjusted with genetic programming. The equations developed in this study were used to predict the fresh performance of the paste. The fresh behaviour of the mortar was predicted with the equations adjusted in a previous work [32]. The mortar used the same materials in its paste design, and a sand to mortar volume ratio of 0.475 was fixed in its mix proportioning [33].

Marsh cone time (paste parameter) predicted according to Eq. (2) was therefore confronted with the Tfunnel (mortar parameter) estimated using an equation adjusted (Eq. 7) in a previous work [32]. In the mortar study [32], the fresh state behaviour was analysed using empirical tests (Dflow and Tfunnel, but not yield stress), so the dimensionless yield stress was calculated using the Dflow measurements to analyse the relationship between the yield stress of both the paste and the mortar. For this purpose, the equation proposed by Li et al. [42], Eq. (5), was used.

$$\tau_y^{'} = \exp\left(-1.0782 \bullet D_s^{'} - 0.1286\right) \quad \text{Eq. 5}$$

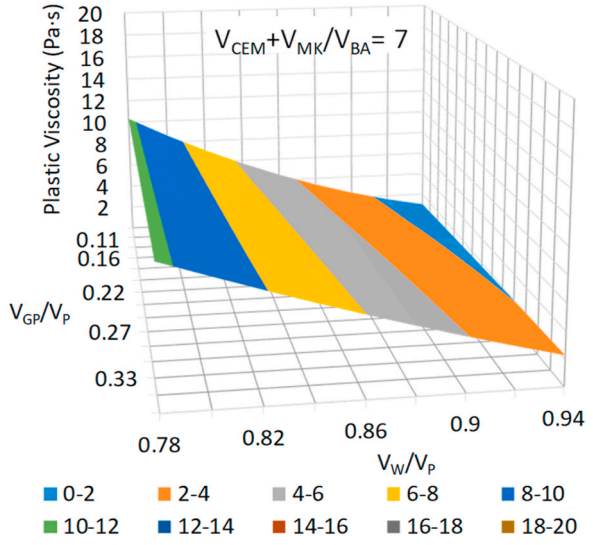

Fig. 19. V_{GP}/V_P influence on plastic viscosity.

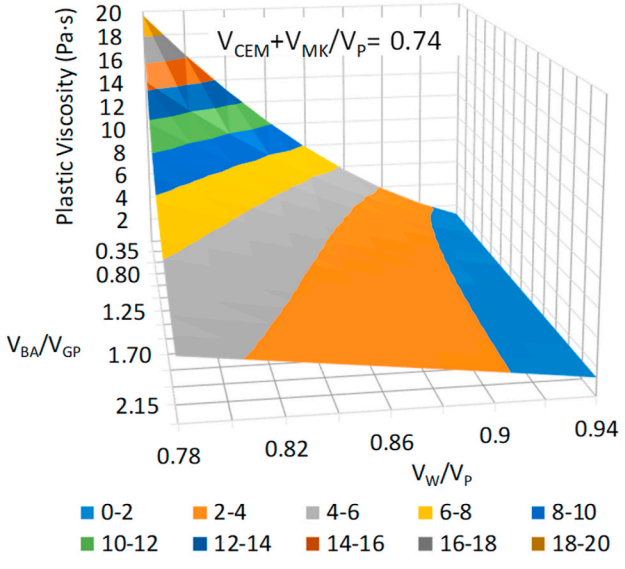

Fig. 20. V_{BA}/V_{GP} influence on plastic viscosity.

In Eq. (5), D'_s is the dimensionless spread diameter. It was calculated as a relationship between the spread diameter measured in test (D_s) and the diameter of the slump device (D_{base}), so $D'_s = D_s/D_{base}$.

The yield stress of the paste (which was predicted using Eq. (4)) was compared to the dimensionless yield stress of the mortar obtained with Eq. (5) and Dflow results [32].

Figs. 21 and 22 show the relationship between Marsh cone time (paste) and Tfunnel (mortar), as well as the relationship between the yield stress of the paste and the yield stress of the mortar (calculated according to the adjusted equations), respectively.

Figures are composed of eight data series that correspond with eight representative mixes obtained from the previous parametric analysis. In other words, the blue series correspond to mixes where the effect of $V_{CEM} + V_{MK}/V_P$ when $V_{BA}/V_P = 1$, which was kept constant, was studied. Light blue points correspond to the mix where $V_{CEM} + V_{MK}/V_P = 0.632$, and dark blue to the mix where $V_{CEM} + V_{MK}/V_P = 0.764$ (first and last point of the analysed range of $V_{CEM} + V_{MK}/V_P$). Similarly, the orange series correspond to mixes where the V_{BA}/V_P variations were analysed when the $(V_{CEM} + V_{MK})/V_{GP}$ ratio was fixed at 3. The light orange is the mix where V_{BA}/V_P was 0.126, and the dark orange is the mix where this ratio was 0.070 (again the two extreme values that defined the range of this ratio in the parametric analysis). The two grey series were selected from the analysis of the effect of changes on V_{GP}/V_P when fixed $(V_{CEM} + V_{MK})/V_{BA} = 7$. In this case, light grey fixes V_{GP}/V_P at 0.362, and dark grey at 0.110. Finally, the two green series correspond to mixes

Table 8
Effects on paste properties.

	CEM MK ↑BA GP W	CEM MK BA ↑GP W	CEM MK ↑BA GP W	CEM MK BA ↑GP W
MC	↑ 8.8%	↑ 38.9%	↑ 2.1%	↑ 10.9%
YS	↓ 3.9%	↑ 19.9%	↓ 1.8%	↓ 3.9%
PV	↑ 53.5%	↑ 55.3%	↓ 59.7%	↑ 0.6%

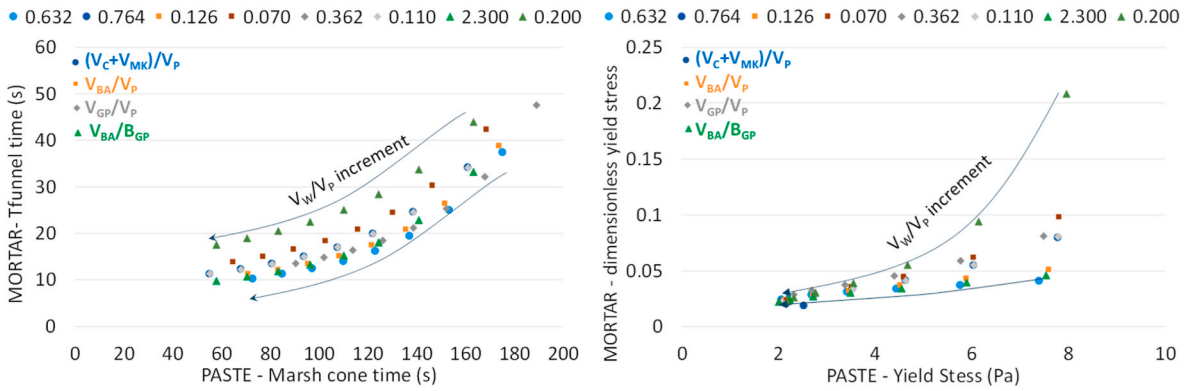

Fig. 21. Marsh cone time of the paste vs Tfunnel of the mortar.

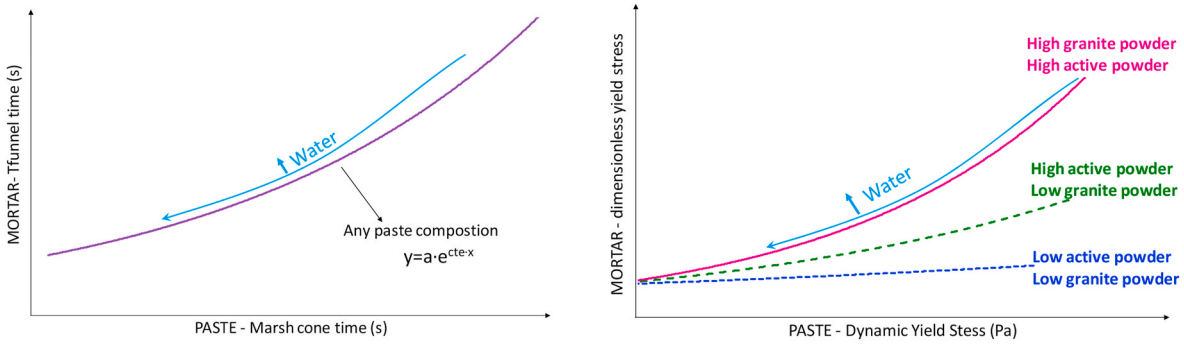

Fig. 22. Yields stress of the paste vs dimensionless yield stress of the mortar.

obtained when V_{BA}/V_{GP} variations were analysed keeping the ratio controlling active powders, $V_{CEM} + V_{MK}/V_P$, fixed at 0.74. The light green points were obtained by fixing V_{BA}/V_{GP} at 2.300, and the dark green ones at 0.200.

Water volume was the main parameter affecting fresh behaviour, so the points of each series were obtained varying V_W/V_P from 0.78 to 0.94.

Fig. 21 shows that the function relating the Tfunnel of the mortar and the Marsh cone time of the paste followed the same trend in all mixes regardless the composition of the binders used. The function was exponential, and the exponent that controlled the slope of the curve was maintained in the different series. Despite the various binder types, all curves were parallel. This exponential relationship indicated that, when water volume was high, changes in Marsh cone time of the paste slightly affected the Tfunnel of the mortar, and when water volume was low, changes in Marsh cone time significantly varied the Tfunnel of the mortar.

When the amount of water was high, the effect of the interaction between sand particles on the mortar was small, so increases in the

Marsh cone time of the pastes slightly affected when this paste was transferred to a mortar. The rheological behaviour of the mortar was controlled by the rheological behaviour of the paste. For example, if the light blue curve were analysed, an increase in Marsh cone time of 17% would increase the Tfunnel of the mortar only by 2%. However, in the same blue series, when water volume was low, an increase in Marsh cone time of 12% also increased the Tfunnel of the mortar by 35%. The interaction between the sand particles introduced into the mortar was large, thus becoming the dominating factor that controlled the fresh behaviour of the mortar when water volume was low.

Fig. 22 shows that the relationship between the yield stress of both the paste and the mortar depends on the binder composition (the curves are not parallel) when water volume varies. Mixes with low content of active fines (light blue on opposition to dark blue) or with fines with good geometrical properties, not very rough or angular (light green on opposition to dark green), showed relationships where the yield stress of the paste highly increased (22%), and that of the mortar was slightly modified (11%). However, when the volume of active fines (dark blue) or of powder materials with poor geometrical properties (dark green) increased, the changes in the yield stress of the paste significantly modified the yield stress of the mortar. This effect was accentuated when V_W/V_P was low (the right area of each series), observing in 0.2 dark green series that increases in the yield stress of 22% in the paste corresponded in the mortar with increases in the yield stress of more than 50%.

Fig. 23 shows that, when water volume was high, changes in Marsh cone time or in the yield stress of the paste slightly changed the rheological parameter of the mortar. However, when water volume was low, a small change in the paste behaviour significantly changed mortar performance. The exponential trend obtained with the Marsh cone and Tfunnel was similar regardless of the paste composition.

On the contrary, the relationship between the yield stress of the paste and the yield stress of the mortar was different in each mix. Mixes with low active powders or with powder materials with good geometrical properties presented an exponential curve with a lower slope than when the volume of angular or rough particles was high, so even when water content was low, changing paste performance hardly affected mortar behaviour.

7. Conclusions

This study develops an experimental plan of 25 paste mixes developed by a central composite design with quaternary binders. Genetic programming was applied to the results concluding that this technique, unlike other evolutionary computation techniques, has made it possible to understand the fresh behaviour of the cement pastes and to translate it into mathematical expressions or predictive models that explicitly link the variables used with the properties measured in the experimental tests. In this manner, suitable models (whose performance has been confirmed with statistical parameters) have been obtained that predict the Marsh Cone, the plastic viscosity (PV) and the yield stress (YS) of the cement paste.

Afterwards, a parametric analysis was carried out to analyse the influence of the main mixing parameter and of the new by-products on the studied properties, thus leading to the following conclusions.

- After analysing the studied factors affecting paste rheology, it was concluded that the most important parameter affecting fresh behaviour was V_w/V_p because all fresh parameters significantly changed when it varied.
- After comparing biomass ash and granite powder, it was concluded that granite powder with particles whose geometrical properties were worse than biomass ash affected the fresh properties of the paste more negatively than biomass ash (the yield stress and the plastic viscosity were reduced).
- In general, Marsh cone time was significantly affected by particle interaction, while the yield stress was more affected by water demand. Plastic viscosity was dominated by water demand when water content was low and was affected by the particle interaction when water volume was high.

The rheological parameters obtained in pastes and mortars with the same dosages when changing water volume were compared. The relationship between the fresh state parameter of the paste and the fresh state parameter of the mortar followed an exponential trend. However, the curves obtained for all mixes were parallel for Marsh cone and Tfunnel, while the trend was different in the yield stress and depended on the geometrical properties of the binder composition, with the slope of the curve being high when the particles

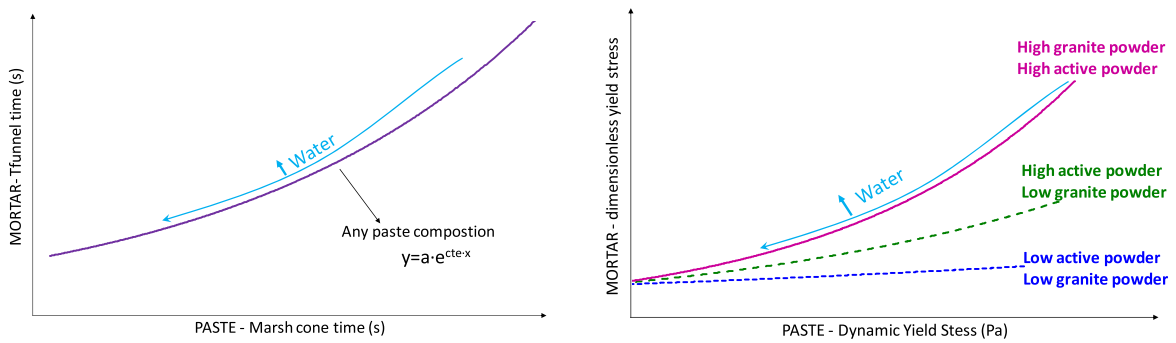

Fig. 23. Schematic behaviour of the paste-mortar relationship.

of the powder materials showed bad geometrical properties.

Finally, genetic programming is an effective tool to analyse the influence of many parameters on the fresh behaviour of cement-based materials and allows engineers to adjust models for their study. This kind of tools is suggested especially when the design of cement-based mortar/concretes includes new raw materials.

CRediT authorship contribution statement

Gemma Rojo-López: Writing – original draft, Validation, Methodology, Investigation, Formal analysis. **Belén González-Fonteboa:** Writing – review & editing, Validation, Supervision, Investigation, Funding acquisition, Formal analysis, Conceptualization. **Juan Luis Pérez-Ordóñez:** Writing – review & editing, Validation, Methodology, Formal analysis. **Fernando Martínez-Abella:** Writing – review & editing, Supervision, Investigation, Conceptualization.

Declaration of competing interest

The authors declare that they have no known competing financial interests or personal relationships that could have appeared to influence the work reported in this paper.

Data availability

Data will be made available on request.

Acknowledgements

This study is part of two projects entitled: “Design of sustainable concrete for 3D printing based on rheology and on the control of very early properties (Eco3DConcrete)- PID2020-115433RB-I00”, “Design of concrete precast elements incorporating sustainable strategies for self-healing to increase their service life (PREHEALING)- PDC2021-121660-I00” and "Exploiting the synergic effects between 3D printing and self-healing technologies to design sustainable and durable concrete (3DHealConcrete) - TED2021-129757B–I00" funded by MINECO.

References

[1] K.L. Scrivener, V.M. John, E.M. Gartner, Eco-efficient cements: potential economically viable solutions for a low-CO2 cement-based materials industry, Cem. Concr. Res. 114 (2018) 2–26, https://doi.org/10.1016/j.cemconres.2018.03.015.
[2] A. Pandey, B. Kumar, Utilization of agricultural and industrial waste as replacement of cement in pavement quality concrete: a review, Environ. Sci. Pollut. Res. 29 (2022) 24504–24546, https://doi.org/10.1007/S11356-021-18189-5.
[3] Y. Han, R. Lin, X.Y. Wang, Performance and sustainability of quaternary composite paste comprising limestone, calcined Hwangtoh clay, and granulated blast furnace slag, J. Build. Eng. 43 (2021) 102655, https://doi.org/10.1016/J.JOBE.2021.102655.
[4] M. Frías, M.I. S, Granite quarry waste as a future eco-ef fi cient supplementary cementitious material (SCM): Scienti fi c and technical considerations, 148, https://doi.org/10.1016/j.jclepro.2017.02.048, 2017.
[5] K. Sobolev, M. Kozhukhova, K. Sideris, E. Menéndez, M. Santhanam, Alternative supplementary cementitious materials, RILEM State-of-the-Art Reports 25 (2018) 233–282, https://doi.org/10.1007/978-3-319-70606-1_7.
[6] J.M. Paris, J.G. Roessler, C.C. Ferraro, H.D. DeFord, T.G. Townsend, A review of waste products utilized as supplements to Portland cement in concrete, J. Clean. Prod. 121 (2016) 1–18, https://doi.org/10.1016/j.jclepro.2016.02.013.
[7] E. Aprianti S, A huge number of artificial waste material can be supplementary cementitious material (SCM) for concrete production – a review part II, J. Clean. Prod. 142 (2017) 4178–4194, https://doi.org/10.1016/j.jclepro.2015.12.115.
[8] R. Saleh Ahari, T. Kemal Erdem, K. Ramyar, Effect of various supplementary cementitious materials on rheological properties of self-consolidating concrete, Constr. Build. Mater. 75 (2015) 89–98, https://doi.org/10.1016/j.conbuildmat.2014.11.014.
[9] T.V. Fonseca, M.A.S. dos Anjos, R.L.S. Ferreira, F.G. Branco, L. Pereira, Evaluation of self-compacting concretes produced with ternary and quaternary blends of different SCM and hydrated-lime, Constr. Build. Mater. 320 (2022) 126235, https://doi.org/10.1016/J.CONBUILDMAT.2021.126235.
[10] M. Gesoğlu, E. Güneyisi, M.E. Kocabağ, V. Bayram, K. Mermerdaş, Fresh and hardened characteristics of self compacting concretes made with combined use of marble powder, limestone filler, and fly ash, Constr. Build. Mater. 37 (2012) 160–170, https://doi.org/10.1016/j.conbuildmat.2012.07.092.
[11] Ö. Biricik, B. Aytekin, A. Mardani, Effect of waste binder material usage rate on thixotropic behaviour of cementitious systems, Constr. Build. Mater. 403 (2023), https://doi.org/10.1016/j.conbuildmat.2023.133197.
[12] S. Nunes, C. Costa, Numerical optimization of self-compacting mortar mixture containing spent equilibrium catalyst from oil refinery, J. Clean. Prod. 158 (2017) 109–121, https://doi.org/10.1016/j.jclepro.2017.04.161.
[13] S. Nunes, A.M. Matos, T. Duarte, H. Figueiras, J. Sousa-Coutinho, Mixture design of self-compacting glass mortar, Cem. Concr. Compos. 43 (2013) 1–11, https://doi.org/10.1016/j.cemconcomp.2013.05.009.
[14] A.M. Matos, L. Maia, S. Nunes, P. Milheiro-Oliveira, Design of self-compacting high-performance concrete: study of mortar phase, Constr. Build. Mater. 167 (2018) 617–630, https://doi.org/10.1016/j.conbuildmat.2018.02.053.
[15] J.P. Moretti, S. Nunes, A. Sales, Self-compacting concrete incorporating sugarcane bagasse ash, Constr. Build. Mater. 172 (2018) 635–649, https://doi.org/10.1016/j.conbuildmat.2018.03.277.
[16] D. Gueciouer, G. Youcef, N. Tarek, Rheological and Mechanical Optimization of a Steel Fiber Reinforced Self-Compacting Concrete Using the Design of Experiments Method, vol. 26, 2019, pp. 1097–1117, https://doi.org/10.1080/19648189.2019.1697758.
[17] T. Naadia, Y. Ghernouti, D. Gueciouer, Development of a measuring procedure of rheological behavior for self compacting concrete, J. Adv. Concr. Technol. 18 (2020) 328–338, https://doi.org/10.3151/JACT.18.328.
[18] R.S. Ahari, T.K. Erdem, K. Ramyar, Thixotropy and structural breakdown properties of self consolidating concrete containing various supplementary cementitious materials, Cem. Concr. Compos. 59 (2015) 26–37, https://doi.org/10.1016/j.cemconcomp.2015.03.009.
[19] I.-C. Yeh, Modeling slump flow of concrete using second-order regressions and artificial neural networks, Cem. Concr. Compos. 29 (2007) 474–480, https://doi.org/10.1016/j.cemconcomp.2007.02.001.
[20] J.L. Pérez, A. Cladera, J.R. Rabuñal, F. Martínez-Abella, Optimization of existing equations using a new Genetic Programming algorithm: Application to the shear strength of reinforced concrete beams, Adv. Eng. Softw. 50 (2012) 82–96, https://doi.org/10.1016/j.advengsoft.2012.02.008.

[21] G. Abdollahzadeh, E. Jahani, Z. Kashir, Genetic programming based formulation to predict compressive strength of high strength concrete, Civ. Eng. Infrastructures J. 50 (2017) 207–219, https://doi.org/10.7508/ceij.2017.02.001.
[22] J.-S. Chou, C.-F. Tsai, A.-D. Pham, Y.-H. Lu, Machine learning in concrete strength simulations: multi-nation data analytics, Constr. Build. Mater. 73 (2014) 771–780, https://doi.org/10.1016/j.conbuildmat.2014.09.054.
[23] I. González-Taboada, B. González-Fonteboa, F. Martínez-Abella, J.L. Pérez-Ordóñez, Prediction of the mechanical properties of structural recycled concrete using multivariable regression and genetic programming, Constr. Build. Mater. 106 (2016) 480–499, https://doi.org/10.1016/j.conbuildmat.2015.12.136.
[24] N.S. Piro, A. Salih, S.M. Hamad, R. Kurda, Comprehensive multiscale techniques to estimate the compressive strength of concrete incorporated with carbon nanotubes at various curing times and mix proportions, J. Mater. Res. Technol. 15 (2021) 6506–6527, https://doi.org/10.1016/j.jmrt.2021.11.028.
[25] C. Jin, Y. Qian, S. Ayub Khan, W. Ahmad, F. Althoey, B. Saad Alotaibi, M. Awad Abuhussain, Investigating the feasibility of genetic algorithms in predicting the properties of eco-friendly alkali-based concrete, Constr. Build. Mater. 409 (2023) 134101, https://doi.org/10.1016/j.conbuildmat.2023.134101.
[26] I. Navarrete, I. La Fé-Perdomo, J.A. Ramos-Grez, M. Lopez, Predicting the evolution of static yield stress with time of blended cement paste through a machine learning approach, Constr. Build. Mater. 371 (2023), https://doi.org/10.1016/j.conbuildmat.2023.130632.
[27] I. Navarrete, Y. Kurama, N. Escalona, M. Lopez, Impact of physical and physicochemical properties of supplementary cementitious materials on structural build-up of cement-based pastes, Cem. Concr. Res. 130 (2020) 105994, https://doi.org/10.1016/j.cemconres.2020.105994.
[28] S. Al-Martini, M. Nehdi, Genetic algorithm rheological equations for cement paste, Proc. Inst. Civ. Eng. Constr. Mater. 163 (2010) 77–85, https://doi.org/10.1680/coma.2010.163.2.77.
[29] H. Figueiras, S. Nunes, J.S. Coutinho, C. Andrade, Linking fresh and durability properties of paste to SCC mortar, Cem. Concr. Compos. 45 (2014) 209–226, https://doi.org/10.1016/j.cemconcomp.2013.09.020.
[30] T. Ji, T. Lin, X. Lin, A concrete mix proportion design algorithm based on artificial neural networks, Cem. Concr. Res. 36 (2006) 1399–1408, https://doi.org/10.1016/j.cemconres.2006.01.009.
[31] M.I. Shah, M.F. Javed, F. Aslam, H. Alabduljabbar, Machine learning modeling integrating experimental analysis for predicting the properties of sugarcane bagasse ash concrete, Constr. Build. Mater. 314 (2022) 125634, https://doi.org/10.1016/j.conbuildmat.2021.125634.
[32] G. Rojo-López, B. González-Fonteboa, J. Luis Pérez-Ordóñez, F. Martínez-Abella, Parametric analysis in sustainable self-compacting mortars using genetic programming, Constr. Build. Mater. 404 (2023) 133189, https://doi.org/10.1016/J.CONBUILDMAT.2023.133189.
[33] G. Rojo-López, S. Nunes, B. González-Fonteboa, F. Martínez-Abella, Quaternary blends of portland cement, metakaolin, biomass ash and granite powder for production of self-compacting concrete, J. Clean. Prod. 266 (2020) 121666, https://doi.org/10.1016/j.jclepro.2020.121666.
[34] H.H.C. Wong, A.K.H. Kwan, Packing density of cementitious materials: Part 1-measurement using a wet packing method, Mater. Struct. Constr. 41 (2008) 689–701, https://doi.org/10.1617/s11527-007-9274-5.
[35] Normes Françaises, NF P18-513 Addition for Concrete - Metakaolin - Specifications and Conformity Criteria, 2012.
[36] AENOR, UNE -EN 196-1, Cement Test Methods. Part 1: Determination of Mechanical Resistances, 2005 (in Spanish), Madrid, Spain.
[37] N. Roussel, R. Le Roy, The Marsh cone: a test or a rheological apparatus? Cem. Concr. Res. 35 (2005) 823–830, https://doi.org/10.1016/j.cemconres.2004.08.019.
[38] AENOR, UNE-EN 12715, Execution of special geotechnical works, grouting (2001) (in Spanish), Madrid, Spain.
[39] I. González-Taboada, B. González-Fonteboa, F. Martínez-Abella, D. Carro-López, Self-compacting recycled concrete: relationships between empirical and rheological parameters and proposal of a workability box, Constr. Build. Mater. 143 (2017) 537–546, https://doi.org/10.1016/j.conbuildmat.2017.03.156.
[40] J. Murray, C. Books, On the origin of species by means of natural selection, or the preservation of favoured races in the struggle for life. https://diginole.lib.fsu.edu/islandora/object/fsu:750821, 1859. (Accessed 12 October 2023).
[41] J.R. Koza, Genetic Programming : on the Programming of Computers by Means of Natural Selection, MIT Press, Cambridge, Massachusetts, 1992.
[42] H. Li, A. Wu, H. Cheng, Generalized models of slump and spread in combination for higher precision in yield stress determination, Cem. Concr. Res. 159 (2022) 106863, https://doi.org/10.1016/j.cemconres.2022.106863.